

Pressure-induced quenching of the charge-density-wave state in rare-earth tritellurides observed by x-ray diffraction

A. Sacchetti,¹ C. L. Condon,² S. N. Gvasaliya,³ F. Pfuner,¹ M. Lavagnini,¹ M. Baldini,⁴ M. F. Toney,² M. Merlini,⁵ M. Hanfland,⁵ J. Mesot,³ J.-H. Chu,⁶ I. R. Fisher,⁶ P. Postorino,⁴ and L. Degiorgi¹

¹Laboratorium für Festkörperphysik, ETH-Zürich, CH-8093 Zürich, Switzerland

²Stanford Synchrotron Radiation Laboratory, Stanford Linear Accelerator Center, Menlo Park, California 94025, USA

³Laboratory for Neutron Scattering, ETH Zürich and Paul Scherrer Institute, CH-5232 Villigen, PSI, Switzerland

⁴Dipartimento di Fisica and CNR-INFN-Coherentia, Università "La Sapienza," P.le A. Moro 5, I-00185 Rome, Italy

⁵European Synchrotron Radiation Facility, Boîte Postale 220, F-38043 Grenoble, France

⁶Geballe Laboratory for Advanced Materials and Department of Applied Physics, Stanford University, Stanford, California 94305-4045, USA

(Received 23 March 2009; published 1 May 2009)

We report an x-ray diffraction study on the charge-density-wave (CDW) LaTe_3 and CeTe_3 compounds as a function of pressure. We extract the lattice constants and the CDW modulation wave vector. We observe that the intensity of the CDW satellite peaks tend to zero with increasing pressure, thus providing direct evidence for a pressure-induced quenching of the CDW phase. Our findings further support the equivalence between chemical and applied pressures in $R\text{Te}_3$, put forward by our previous optical investigations, but reveal some subtle differences. We offer a possible explanation for these differences.

DOI: [10.1103/PhysRevB.79.201101](https://doi.org/10.1103/PhysRevB.79.201101)

PACS number(s): 71.45.Lr, 61.05.cp, 62.50.-p

Low dimensionality plays an important role in condensed-matter physics owing to the observation of intriguing phenomena such as the formation of spin- and charge-density waves (CDWs), as well as non-Fermi-liquid behavior of the electronic properties in a variety of materials.^{1,2} A revival of interest in low-dimensional interacting electron gas systems, and in their wealth of astonishing properties, has taken place since the discovery of high-temperature superconductivity in the layered two-dimensional (2D) copper oxides. This furthermore led to the quest for prototype layered systems, allowing a systematic study of these phenomena. In this context, the rare-earth tritellurides ($R\text{Te}_3$, with $R=\text{La-Sm}$ and Gd-Tm) were recently revisited and recognized as a paramount example of easily tunable 2D materials. Their crystal structure is weakly orthorhombic (pseudotetragonal)³⁻⁵ and is composed of corrugated $R_2\text{Te}_2$ slabs alternating with pairs of Te layers, stacked along the (long) b axis. The formation of the CDW condensate, hosted within Te layers, is to a large extent driven by the nesting of the Fermi surface (FS),^{6,7} which is thus gapped over a sizeable portion. Systematic x-ray diffraction (XRD) studies of the $R\text{Te}_3$ series revealed that the modulation vector $\vec{q} \approx (2/7)\vec{c}^*$ (\vec{c}^* is the reciprocal lattice vector of the c axis) is almost the same for every member of this family⁸ and that the CDW state is progressively suppressed as the lattice is chemically compressed (i.e., going from $R=\text{La}$ to $R=\text{Tm}$).⁹ The transition temperature T_{CDW} is 250 K for TmTe_3 , increases gradually up to 410 K in SmTe_3 ,⁹ and is larger than 450 K in the tritellurides with lighter rare-earth elements ($R=\text{La-Nd}$).⁸ A corresponding strong reduction in the CDW gap with chemical pressure was then established on the basis of optical-spectroscopy experiments.¹⁰ Subsequent light-scattering experiments on the same series of compounds showed that the CDW gap reduction is accompanied by a progressive disappearance of the signal from the Raman-active phonon modes.¹¹ The same effects have been observed in the light rare-earth tritellurides

under external hydrostatic pressure: infrared reflectivity experiments on CeTe_3 at high pressures¹² as well as on the related LaTe_2 compound¹³ revealed a pressure-induced reduction in the CDW gap, while the Raman-active phonons in LaTe_3 and CeTe_3 disappeared.¹¹

In this Rapid Communication we present a high-pressure XRD diffraction study on LaTe_3 and CeTe_3 , with the goal of monitoring the evolution of the CDW distortion with pressure. We establish a pressure-induced quenching of the CDW state and show that, while there is general equivalence between physical and chemical pressure, there are also important subtle distinctions. We speculate that this is due to differences in the effective dimensionality, that derive from the chemical and physical lattice compression, and in the role played by fluctuation effects.

The LaTe_3 and CeTe_3 single crystals were grown as described in Ref. 14. Small ($\approx 20 \times 20 \times 10 \mu\text{m}^3$) samples were placed inside the hole (initial diameter 250 μm) of a stainless steel gasket of a membrane driven diamond-anvil cell (DAC) (culet size 600 μm) together with He as pressure transmitting medium and a $\sim 5 \mu\text{m}$ diameter ruby sphere for pressure calibration.¹⁵ Diffraction images were collected at the ID09A beamline of the ESRF with a monochromatic beam ($\lambda=0.413 \text{ \AA}$) focused to $20 \times 20 \mu\text{m}^2$ using a MAR345 image plate detector. During exposure the pressure cells were rotated around the ϕ axis. Here at $\phi=0$ the incident x-rays are along the b axis and ϕ rotates the b axis about the incoming beam direction. Total rotation ranges were 40° with standard 1.5-mm-high diamond anvils and 60° with cells modified for Boehler-Almax anvils.¹⁶ For the low-temperature measurements the DAC was placed inside a He flow cryostat with the rotation range limited to $\pm 5^\circ$. These latter measurements were performed on coarse polycrystalline samples.

XRD patterns were collected at room temperature as a function of pressure for LaTe_3 and CeTe_3 single crystal and

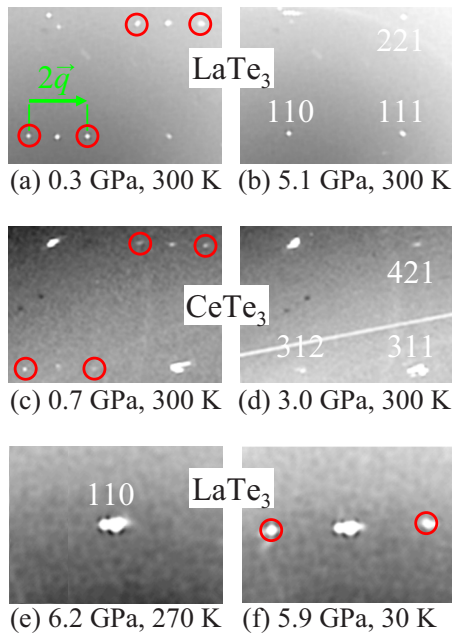


FIG. 1. (Color online) Selected XRD patterns on single-crystals of LaTe_3 at 300 K and at (a) 0.3 GPa and (b) 5.1 GPa, and of CeTe_3 at 300 K and at (c) 0.7 GPa and (d) 3.0 GPa, and finally on polycrystalline LaTe_3 at 270 K and (e) 6.2 GPa, and at 30 K and (f) 5.9 GPa. Circles highlight the CDW satellite peaks. The modulation vector \vec{q} is also shown in (a).

as a function of temperature for a LaTe_3 polycrystal at 6.0 ± 0.2 GPa. Representative areas of the diffraction patterns at selected pressures and temperatures are shown in Fig. 1. From a technical point of view, it is worth emphasizing that the intensity of the satellites varies by a large amount from one fundamental reflection to the other.⁹ Therefore, not all of them were observed in our 2D images. Furthermore, at high pressures cracks of the sample are unavoidable. Since each image is a result of a continuous rotation of the sample around the ϕ axis, we will also catch Bragg peaks from the pieces of the crystals which are slightly misaligned. Moreover, stacking faults may lead to weak scattering intensity at forbidden peaks, as first suggested by DiMasi and co-workers.¹⁷

At low pressure and at 300 K, several Bragg peaks in both LaTe_3 and CeTe_3 display pairs of satellites, which are due to the modulated CDW lattice distortion.⁹ Upon increasing pressure, the intensity of these satellite peaks is progressively reduced and they eventually disappear at high enough pressure (3 and 5 GPa in CeTe_3 and LaTe_3 , respectively) as shown in Figs. 1(a)–1(d). At 6.0 ± 0.2 GPa the satellite peaks in LaTe_3 are recovered by cooling the polycrystalline specimen well below 300 K [see Figs. 1(e) and 1(f)]. This shows that at this pressure the CDW transition occurs at a lower critical temperature T_{CDW} (i.e., < 300 K).

From the positions of selected Bragg peaks we obtained the lattice parameters and thus the unit-cell volume. The corresponding results for CeTe_3 under pressure at 300 K and for LaTe_3 as a function of temperature at 6.0 ± 0.2 GPa are shown in Fig. 2. The pressure experiment on LaTe_3 at room temperature provides similar results (not shown) as for

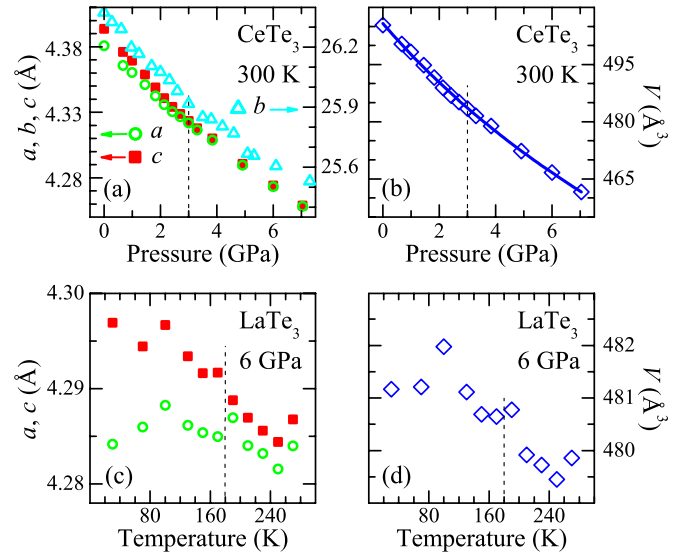


FIG. 2. (Color online) Lattice parameters (left panels) and unit-cell volume (right panels) for CeTe_3 at 300 K [(a) and (b)] as a function of pressure and for LaTe_3 polycrystal at 6.0 ± 0.2 GPa [(c) and (d)] as a function of temperature. The solid line in (b) is the Birch-Murnaghan fit to the data (Ref. 18). Vertical dashed lines indicate the pressure and temperature where the CDW satellite peaks (Fig. 1) disappear.

CeTe_3 . At ambient pressure the slight orthorhombic distortion of the unit-cell results in a small difference between the in-plane lattice parameters a and c .⁵ Upon increasing pressure this difference between the a and c axes decreases, and both lattice parameters become nearly indistinguishable above 3 GPa in CeTe_3 [Fig. 2(a)]. A similar effect is observed in LaTe_3 at 5 GPa and was previously reported for $R\text{Te}_3$ with $R=\text{Sm-Tm}$ on crossing T_{CDW} at ambient pressure.⁹ The unit-cell volume [Fig. 2(b)] decreases smoothly with pressure and follows the Birch-Murnaghan equation of state¹⁸ with the bulk modulus $B_0=59$ GPa and its pressure derivative $B'=5.6$. The fitted B_0 value is in reasonable agreement with a previous estimate¹² from specific-heat data,¹⁹ while B' lies within the typical range of 4–8.²⁰ A change in the temperature dependence of the c and a lattice constants is also observed when lowering the temperature below 180 K in LaTe_3 at 6 GPa [Fig. 2(c)]. While the scatter in the data is more pronounced than in the experiment as a function of pressure at fixed temperature, the tendency for a and c to diverge below 180 K is evident, such as the weak discontinuity in the unit-cell volume [Fig. 2(d)]. The overall temperature dependence of the lattice parameters is very similar to that observed at ambient pressure in the heavy rare-earth tritellurides,⁹ suggesting an analogous impact of both chemical and applied pressures on the structural properties of $R\text{Te}_3$.

The most compelling result of our investigations is the observation that the integrated intensities of the CDW satellite peaks gradually decrease with increasing pressure at 300 K and vanish at 5 and 2.8 GPa in LaTe_3 and CeTe_3 , respectively [Figs. 3(a) and 3(b)]. The resolution of our experiment does not allow us to distinguish small effects in the diffraction peak intensity. Nonetheless, our finding shows that the

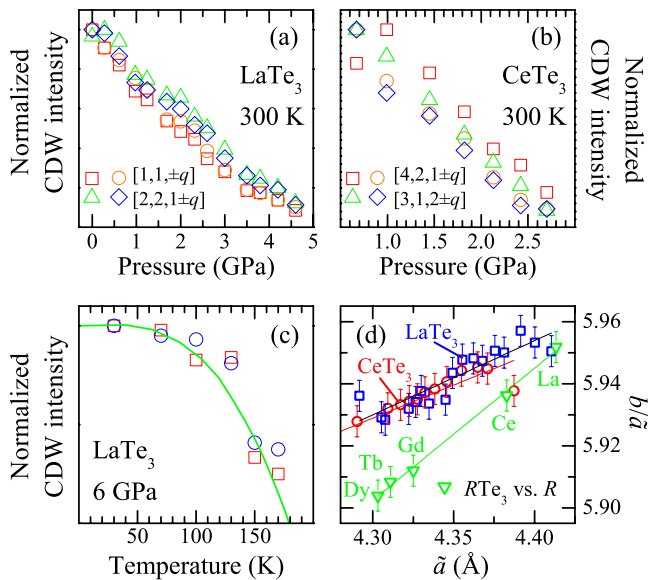


FIG. 3. (Color online) Intensity of selected CDW satellite peaks normalized to a nearby Bragg-peak for (a) LaTe_3 and (b) CeTe_3 at 300 K as a function of pressure and for LaTe_3 at 6.0 ± 0.2 GPa as a function of temperature, with the prediction from the BCS theory (c). (d) Ratio b/\bar{a} (see text) as a function of the average lattice constant \bar{a} . Thin lines in panel (d) are linear interpolations to the data, as guide to the eyes.

CDW state, observed at ambient pressure and 300 K in these compounds, is quenched by a moderate lattice compression of about 5% of the volume. This is moreover consistent with the previously reported pressure-induced reduction in the CDW gap¹² and of the integrated intensities of the Raman-active phonon modes.¹¹ The temperature dependence of the intensities of the CDW satellite peaks of LaTe_3 at 6 GPa [Fig. 3(c)] is also similar to that of the heavy rare-earth tritellurides at ambient pressure,⁹ supporting again a qualitative equivalence between chemical and applied pressure in order to achieve the lattice compression. We note that the satellite intensities are consistent with the BCS behavior²¹ with $T_{\text{CDW}} = 180$ K, bearing a striking similarity with results on prototype one-dimensional (1D) systems.¹

To further test the extent of equivalence between chemical and applied pressure, we first define the average in-plane lattice parameter $\bar{a} = (a+c)/2$, which is related to the Te-Te distance within the Te layers. \bar{a} can be considered as a common variable for several quantities measured upon compressing the lattice. We then plot in Fig. 3(d) the quantity b/\bar{a} , which is representative of the anisotropy ratio between the interplane and intraplane Te-Te distances, for the RTe_3 series^{4,9} and for LaTe_3 and CeTe_3 under applied pressure using the data from Fig. 2(a). Despite some scatter in the data there is a clear trend, showing a significantly more pronounced decrease of b/\bar{a} in the chemical series than in the applied pressure experiment. The \bar{a} dependence of the CDW modulation wave vector $|\vec{q}|$, extracted from the positions of the satellite peaks (Fig. 1), for the RTe_3 series at 300 K (Ref. 8) and for LaTe_3 as a function of pressure is shown in Fig. 4(a). The magnitude of $|\vec{q}|$ monotonously increases with increasing pressure. The similarity of $|\vec{q}|$ with chemical and

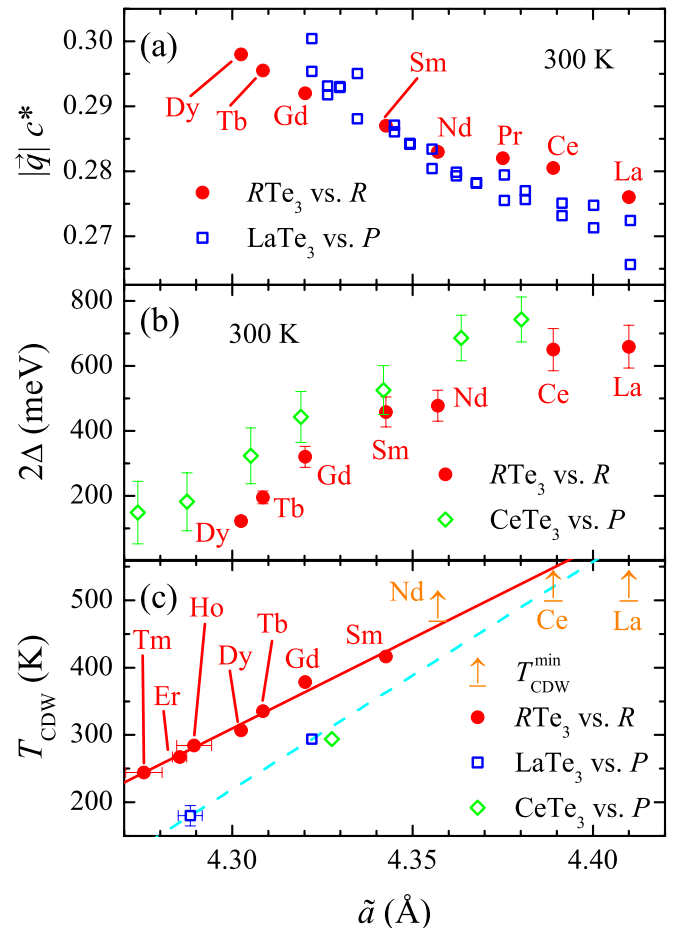


FIG. 4. (Color online) (a) Magnitude of the CDW wave vector \vec{q} and (b) of the CDW gap 2Δ at 300 K for the RTe_3 series and for LaTe_3 and CeTe_3 under applied pressure as a function of the average lattice constant \bar{a} (see text), respectively. Chemical-pressure data in (a) are from Ref. 8 and the 2Δ values in (b) are from Refs. 10 and 12 for RTe_3 and CeTe_3 , respectively. (c) CDW-transition temperature T_{CDW} as a function of \bar{a} for the RTe_3 series^{8,9} and for LaTe_3 and CeTe_3 at high pressures. The solid and dashed lines in (c) are linear fits to the data.

applied pressures is suggestive of an equivalent modification of the FS and thus of its nesting properties,^{7,10} upon compressing the lattice. The \bar{a} dependence of the CDW gap 2Δ (averaged over the FS) for the RTe_3 series at 300 K (Ref. 10) and for CeTe_3 under pressure¹² is shown in Fig. 4(b). The comparison here is much better than that reported in Ref. 12, which was based on a crude estimation of $\bar{a}(P)$. The two data sets follow the same trend and within the experimental error the 2Δ values for both experiments are almost identical. From our data we can furthermore exclude that the CDW gap in the chemical RTe_3 series is larger than in CeTe_3 under pressure. Below we conjecture as to the cause of the pressure dependence of the critical temperature T_{CDW} . From our isothermal experiments at 300 K on LaTe_3 and CeTe_3 we obtain two points in the \bar{a} - T phase diagram and an additional data point is extracted from the isobaric experiment at 6.0 ± 0.2 GPa on LaTe_3 [i.e., converting the pressure at which the satellite peaks disappear into a corresponding lattice constant (Fig. 2)]. These data are then compared in Fig.

4(c) with T_{CDW} of the $R\text{Te}_3$ series measured at ambient pressure.⁹ For $R=\text{La}$, Ce, and Nd only the lower limits of T_{CDW} are known.⁸

While these findings confirm the overall qualitative equivalence between chemical and applied pressure, they show that a subtle difference exists between the two types of lattice compression. In contrast to our observations for 2Δ [Fig. 4(b)], we note that T_{CDW} is systematically larger for the chemical pressure than for applied pressure. This is unexpected. We speculate that such a behavior is due to a difference in the effective dimensionality of the system when compressing the lattice chemically compared with applied pressure: specifically, the effective dimensionality is larger (more three dimensional) for chemical pressure. This intriguing possibility is consistent with the observation that the relative change of b/\tilde{a} between LaTe_3 and DyTe_3 at ambient pressure is roughly a factor 2 larger than, for instance, in LaTe_3 between 0 GPa (Ref. 9) and 5.5 GPa, for which \tilde{a} is the same as in DyTe_3 at ambient pressure [Fig. 3(d)]. The lower effective dimensionality achieved by applied pressure implies stronger fluctuations and therefore a reduced transition temperature. Based on Fig. 3(d), this predicts that at ambient pressure fluctuation effects (e.g., the diffuse scattering above the transition temperature) should be more important and prominent for the lighter rare earths (larger b/\tilde{a}) than for the heavier rare earths. Our speculative scenario, accounting for the subtle differences between the two types of lattice compressions, merits further investigations, including a detailed structural study of the internal atomic coordinates in the unit cell as a function of applied pressure. None-

theless, a crude linear extrapolation of the T_{CDW} data with chemical pressure and with applied pressure on LaTe_3 [Fig. 4(c)] leads to an intersection at $\tilde{a} \approx 4.43 \text{ \AA}$, which compares nicely with the zero-pressure value for LaTe_3 .⁴

In summary, we have reported a high-pressure XRD study on the CDW LaTe_3 and CeTe_3 compounds. The pressure dependence of the in-plane lattice parameters is consistent with a pressure-induced reduction in the pseudotetragonal phase, i.e., of the lattice distortion accompanying the formation of the CDW condensate. This is similar to what has been observed upon cooling across the CDW transition in LaTe_3 at high pressure (present work), as well as at ambient pressure in the heavy rare-earth tritellurides.⁹ More striking evidence of the pressure-induced quenching of the CDW phase is provided by the vanishing intensities of the CDW satellite peaks with increasing pressure. Such observations supply a compelling support to ideas based on the equivalence between chemical and applied pressures in $R\text{Te}_3$, put forward in our previous work.¹⁰⁻¹²

The authors wish to thank R. Monnier for fruitful discussions. This work was supported by the Swiss National Foundation for the Scientific Research as well as by the NCCR MaNEP pool and also by the (U.S.) Department of Energy, Office of Basic Energy Sciences under Contract No. DE-AC02-76SF00515. Portions of this research were carried out at the Stanford Synchrotron Radiation Laboratory, a national user facility operated by Stanford University on behalf of the U.S. Department of Energy, Office of Basic Energy Sciences.

¹G. Grüner, *Density Waves in Solids* (Addison Wesley, Reading, MA, 1994).

²*Strong Interactions in Low Dimensions*, edited by D. Baeriswyl and L. Degiorgi (Kluwer Academic Publishers, Dordrecht, 2004).

³B. K. Norling and H. Steinfink, *Inorg. Chem.* **5**, 1488 (1966).

⁴P. Villars and L. D. Calvert, *Pearson's Handbook of Crystallographic Data for Intermetallic Phases* (American Society for Metals, Metals Park, OH, 1991).

⁵The crystal structure of $R\text{Te}_3$ belongs to the $Cmcm$ space group,³ which is orthorhombic. However, the in-plane lattice constants a and c differ by approximately $(c-a)/a \sim 0.3\%$ and 0.5% in CeTe_3 and LaTe_3 , respectively (in the standard space-group setting, the b axis is perpendicular to the Te planes).

⁶E. DiMasi, M. C. Aronson, J. F. Mansfield, B. Foran, and S. Lee, *Phys. Rev. B* **52**, 14516 (1995).

⁷V. Brouet, W. L. Yang, X. J. Zhou, Z. Hussain, N. Ru, K. Y. Shin, I. R. Fisher, and Z. X. Shen, *Phys. Rev. Lett.* **93**, 126405 (2004).

⁸C. D. Malliakas and M. G. Kanatzidis, *J. Am. Chem. Soc.* **128**, 12612 (2006).

⁹N. Ru, C. L. Condon, G. Y. Margulis, K. Y. Shin, J. Laverock, S. B. Dugdale, M. F. Toney, and I. R. Fisher, *Phys. Rev. B* **77**, 035114 (2008).

¹⁰A. Sacchetti, L. Degiorgi, T. Giamarchi, N. Ru, and I. R. Fisher,

Phys. Rev. B **74**, 125115 (2006).

¹¹M. Lavagnini, M. Baldini, A. Sacchetti, D. Di Castro, B. Delley, R. Monnier, J.-H. Chu, N. Ru, I. R. Fisher, P. Postorino, and L. Degiorgi, *Phys. Rev. B* **78**, 201101(R) (2008).

¹²A. Sacchetti, E. Arcangeletti, A. Perucchi, L. Baldassarre, P. Postorino, S. Lupi, N. Ru, I. R. Fisher, and L. Degiorgi, *Phys. Rev. Lett.* **98**, 026401 (2007).

¹³M. Lavagnini, A. Sacchetti, L. Degiorgi, E. Arcangeletti, L. Baldassarre, P. Postorino, S. Lupi, A. Perucchi, K. Y. Shin, and I. R. Fisher, *Phys. Rev. B* **77**, 165132 (2008).

¹⁴N. Ru and I. R. Fisher, *Phys. Rev. B* **73**, 033101 (2006).

¹⁵H. K. Mao, J. Xu, and P. M. Bell, *J. Geophys. Res.* **91**, 4673 (1986).

¹⁶R. Boehler and K. De Hantsetters, *High Press. Res.* **24**, 391 (2004).

¹⁷E. DiMasi, B. Foran, M. C. Aronson, and S. Lee, *Chem. Mater.* **6**, 1867 (1994).

¹⁸F. D. Murnaghan, *Proc. Natl. Acad. Sci. U.S.A.* **30**, 244 (1944).

¹⁹K. Y. Shin, V. Brouet, N. Ru, Z. X. Shen, and I. R. Fisher, *Phys. Rev. B* **72**, 085132 (2005).

²⁰S. Jiuxun, W. Qiang, C. Lingcang, and J. Fuqian, *J. Phys. Chem. Solids* **66**, 773 (2005).

²¹M. Tinkham, *Introduction to Superconductivity*, 2nd ed. (McGraw-Hill, New York, 1996).